

# Reactions of Laser Ablated Rhodium Atoms with Nitrogen Atoms and Molecules. Infrared Spectra and Density Functional Calculations on Rhodium Nitrides and Dinitrogen Complexes

Angelo Citra and Lester Andrews\*

Department of Chemistry, University of Virginia, Charlottesville, Virginia 22901

Received: December 4, 1998; In Final Form: February 11, 1999

Laser ablated rhodium atoms mixed with pure  $N_2$  and  $Ar/N_2$  during condensation at 8–10 K produced and trapped several rhodium nitride products and rhodium dinitrogen complexes. The Rh–N vibrations of new product molecules were characterized by nitrogen 14/15 isotopic ratios and intensity patterns.  $RhN$  and  $NRhN$  were observed in both solid nitrogen and argon. Molecules containing two rhodium atoms, including  $Rh_2N$ ,  $Rh_2N_2$ , and  $RhRhN$ , make an important contribution to the overall product yield. Density functional calculations provide support for the vibrational assignments.

## Introduction

The interaction of nitrogen with transition metals is relevant to the study of nitrogen fixation. This is achieved industrially by reacting hydrogen and nitrogen at high temperature and pressure over an iron-based catalyst. However, it is also achieved naturally under far milder conditions in several forms of bacteria. Rhizobium, for example, is responsible for the fixation of over 100 million tons of nitrogen annually, more than is achieved industrially, where the enzyme responsible contains molybdenum.<sup>1</sup> This study investigates the reaction between another second row transition metal, rhodium, and nitrogen, in both argon and nitrogen matrixes at cryogenic temperatures. The products identified in this study may provide simple models for larger complexes that could be used in nitrogen fixation. The reaction of laser ablated cobalt atoms with dinitrogen has previously been studied in this laboratory, and the nitrides  $CoN$ ,  $Co_2N$ ,  $Co_2N_2$ , and  $CoCoN$  were characterized.<sup>2</sup>

The reaction between rhodium atoms and dinitrogen has been studied previously using matrix isolation technique.<sup>3</sup> In that work rhodium was produced by thermal evaporation, and the only reaction products observed were the dinitrogen complexes  $Rh(N_2)_n$  ( $n = 1$  to 4). In this work rhodium atoms are produced by laser ablation of a rhodium target, and the high energy atoms this technique generates are able to rupture even the strong triple bond in  $N_2$ , giving rise to several new rhodium nitride products.

## Experimental Section

The techniques for laser ablation and FTIR matrix investigation have been described previously.<sup>4</sup> Rhodium (Goodfellow) was mounted on a rotating (1 rpm) stainless steel rod. The Nd:YAG laser fundamental (1064 nm, 10 Hz repetition rate, 10 ns pulse width) was focused on the target through a hole in the cryogenic window. Laser power ranged from 40 to 60 mJ/pulse at the target. Metal atoms were co-deposited with pure nitrogen and with 4% nitrogen in argon at 2–4 mmol/h for 0.5–1.5 h periods onto the CsI substrate maintained at 8 K. Scrambled isotopic nitrogen was generated by passing the matrix gas containing  $^{14}N_2$  and  $^{15}N_2$  through a microwave discharge prior to condensation with metal atoms. FTIR spectra were recorded with 0.5  $cm^{-1}$  accuracy on a Nicolet 550 spectrometer. Matrix

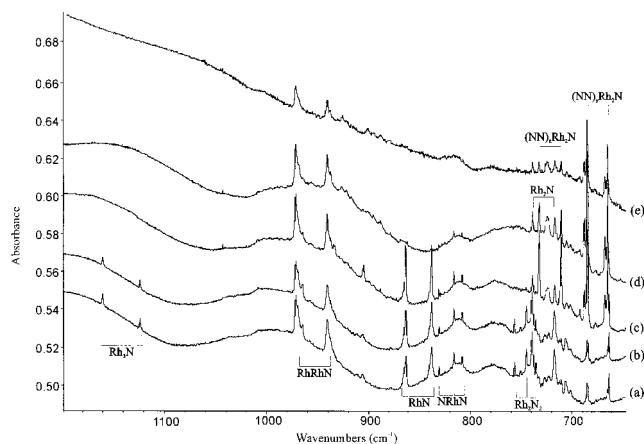


**Figure 1.** Infrared spectra in the 1200–650  $cm^{-1}$  region for laser ablated rhodium atoms co-deposited with isotopically scrambled nitrogen: (a) after 65 min deposition; (b) after 25 min photolysis; (c) after annealing to 30 K; (d) after annealing to 34 K; (e) after annealing to 37 K.

samples were subjected to annealing cycles to promote controlled diffusion and to photolysis by a medium-pressure mercury arc (Phillips, 175 W with globe removed, 240–580 nm).

## Results

Infrared spectra recorded for rhodium and pure dinitrogen or dinitrogen diluted in argon co-deposited at 8 K and the results of DFT calculations will be presented.

**Pure Dinitrogen.** New bands are observed in the region 1200–650  $cm^{-1}$  at 1160.4, 971.5, 863.7, 830.9, 756.7, 739.2/732.3, and 687.3/684  $cm^{-1}$ . The deposition, photolysis, and annealing spectra in this region for the  $^{14}N_2 + ^{14}N^{15}N + ^{15}N_2$  scrambled isotopic experiment are shown in Figure 1, and product absorptions are listed in Table 1. The weak 1160.4  $cm^{-1}$  band is completely destroyed on annealing to 30 K. The 971.5  $cm^{-1}$  band is diminished by photolysis and grows significantly at 30 K, but then decreases on higher temperature annealing. The 863.7  $cm^{-1}$  band increases on photolysis and on annealing

**TABLE 1: Infrared Absorptions (cm<sup>-1</sup>) from Co-deposition of Laser Ablated Rhodium Atoms with Pure Dinitrogen**

<sup>14</sup> N <sub>2</sub>	<sup>15</sup> N <sub>2</sub>	<sup>14</sup> N <sub>2</sub> + <sup>15</sup> N <sub>2</sub>	<sup>14</sup> N <sub>2</sub> + <sup>14</sup> N <sup>15</sup> N + <sup>15</sup> N <sub>2</sub>	R(14/15)	assignment
2202.2	2129.0	<i>a</i>	<i>a</i>	1.0344	Rh(NN) <sub>4</sub>
2178.2	2105.6	<i>a</i>	<i>a</i>	1.0345	Rh(NN) <sub>4</sub>
2003.4	1937.6	2003.4, 1992.9, 1948.8, 1937.4	2003.2, 1992.8, 1981.8, 1959.5, 1948.7, 1937.4	1.0339	N <sub>3</sub> <sup>-</sup>
1771.5	1734.7	1771.5, 1734.7	1771.5, 1734.7	1.02121	RhNO (site)
1765.9	1729.5	1765.9, 1729.5	1765.9, 1729.5	1.02105	RhNO
1765.1	1707.1	1765.1, 1707.1	1765.1, 1735.9, 1707.1	1.03398	Rh <sub>2</sub> (N <sub>2</sub> )
1657.6	1603.4	1657.7, 1649.4, 1613.0, 1603.3	1657.8, 1649.4, 1640.1, 1621.6, 1613.0, 1603.4	1.0337	N <sub>3</sub>
1160.5	1123.4	1160.5, 1123.4	1160.5, 1123.4	1.03303	Rh <sub>3</sub> N
971.7	941.1	971.7, 941.1	971.7, 941.1	1.03252	RhRhN
969.0	937.7	969.0, 937.7	969.0, 937.7	1.03338	RhRhN (site)
964.7	934.2	964.7, 934.2	964.7, 934.2	1.03265	RhRhN (site)
906.6	906.6	906.6	906.6		ORhO
865.8	840.2	865.8, 840.2	865.8, 840.2	1.03047	(NN) <sub>x</sub> RhN (site)
863.5	838.1	863.5, 838.1	863.5, 838.1	1.03031	(NN) <sub>x</sub> RhN
830.9	808.0	830.9, 808.0	830.9, 816.2, 808.0	1.02834	NRhN
756.7	735.6	756.7, 745.0, 735.6	756.7, 745.0, 735.6	1.02868	Rh <sub>2</sub> N <sub>2</sub>
738.9	716.8	738.8, 716.8	738.8, 716.9	1.03083	Rh <sub>2</sub> N
732.5	710.1	732.3, 710.2	732.3, 710.2	1.03154	(NN) <sub>x</sub> Rh <sub>2</sub> N
687.5	666.5	687.3, 666.8	687.3, 666.8	1.03151	(NN) <sub>x</sub> Rh <sub>2</sub> N (site)
684.7	663.8	684.3, 664.0	684.3, 664.0	1.03149	(NN) <sub>x</sub> Rh <sub>2</sub> N

<sup>a</sup> Intermediate components in ref 3.

**TABLE 2: Infrared Absorptions (cm<sup>-1</sup>) from Co-deposition of Laser Ablated Rhodium Atoms with Dinitrogen in Argon (4%)**

<sup>14</sup> N <sub>2</sub>	<sup>15</sup> N <sub>2</sub>	<sup>14</sup> N <sub>2</sub> + <sup>15</sup> N <sub>2</sub>	<sup>14</sup> N <sub>2</sub> + <sup>14</sup> N <sup>15</sup> N + <sup>15</sup> N <sub>2</sub>	R(14/15)	assignment
2197.0	2123.9	<i>a</i>	<i>a</i>	1.03442	Rh(NN) <sub>3</sub> (site)
2193.2	2120.1	<i>a</i>	<i>a</i>	1.03448	Rh(NN) <sub>3</sub>
2188.2	2115.6	<i>a</i>	<i>a</i>	1.03432	Rh(NN) <sub>3</sub> (site)
2185.8	2112.8	<i>a</i>	<i>a</i>	1.03455	Rh(NN) <sub>2</sub>
2178.3	2105.2	<i>a</i>	<i>a</i>	1.03472	Rh(NN) <sub>4</sub> (site)
2174.8	2102.3	<i>a</i>	<i>a</i>	1.03449	Rh(NN) <sub>4</sub>
2153.3	2081.8	<i>a</i>	<i>a</i>	1.03435	Rh(NN)
1775.1	1738.8	1775.1, 1738.8	1775.1, 1738.8	1.02088	RhNO
1763.7	1706.3	1763.7, 1735.0, 1706.3	1763.7, 1706.3 <sup>b</sup>	1.03364	(Rh <sub>2</sub> (N <sub>2</sub> ))
1756.2	1697.3	1756.2, 1697.3	1756.2, 1697.3	1.03547	(Rh <sub>2</sub> (N <sub>2</sub> ) site)
975.6	944.0	975.6, 944.0	975.6, 944.0	1.03347	RhRhN
894.9	868.4	894.9, 868.4	894.9, 868.4	1.03052	RhN
872.9	846.9	872.9, 846.9	872.9, 846.9	1.03070	(NN) <sub>x</sub> RhN
865.2	839.8	865.2, 839.8	865.2, 839.8	1.03025	(NN) <sub>x</sub> RhN
822.8	800.4	822.8, 800.4	822.8, 808.6, 800.4	1.02813	NRhN
748.1	727.0	748.1, 727.0	<i>b</i>	1.02902	Rh <sub>2</sub> N <sub>2</sub>
741.5	719.3	741.5, 719.3	<i>b</i>	1.03086	
728.0	704.9	728.0, 704.9	<i>b</i>	1.03277	Rh <sub>2</sub> N
683.4	662.6	683.4, 662.6	<i>b</i>	1.03139	(NN) <sub>x</sub> Rh <sub>2</sub> N
593.6	575.5	593.6, 575.5	<i>b</i>	1.03145	
568.7	550.5	568.7, 559.1, 550.5	<i>b</i>	1.03306	
542.6	526.6	542.6, 526.6 <sup>b</sup>	<i>b</i>	1.03038	
441.3	427.7	441.3, 427.7 <sup>b</sup>	<i>b</i>	1.03180	

<sup>a</sup> Intermediate components in ref 3. <sup>b</sup> Absorption too weak to observe intermediate bands.

to 30 K but is completely destroyed on higher temperature annealing. The weak 830.9 cm<sup>-1</sup> band decreases during annealing but is not affected by photolysis. The weak 756.7 cm<sup>-1</sup> band is unaffected by photolysis, but is destroyed on annealing to 30 K. The 739.2 cm<sup>-1</sup> band is sharp and intense and is diminished slightly during photolysis but rapidly on annealing to 30 K. The lower frequency site at 732.3 cm<sup>-1</sup> is not present on deposition but grows in markedly during early annealing, decreasing on annealing to higher temperatures. The 687.3/684.4 cm<sup>-1</sup> bands show a large increase on annealing to 34 K but then decrease on further annealing. In the pure <sup>15</sup>N<sub>2</sub> experiment, these bands are shifted as given in Table 1. Only two bands have intermediate components in either the mixed or scrambled isotopic experiments; the 830.9 cm<sup>-1</sup> and 756.7 cm<sup>-1</sup> bands exhibit 1:2:1 intensity triplets in the scrambled <sup>14</sup>N<sub>2</sub> + <sup>14</sup>N<sup>15</sup>N + <sup>15</sup>N<sub>2</sub> experiment, with the intermediate bands at 816.2 cm<sup>-1</sup> and 745.4 cm<sup>-1</sup>. The intermediate bands are also present in the mixed <sup>14</sup>N<sub>2</sub> + <sup>15</sup>N<sub>2</sub> experiment but they are of approximately equal intensity with the pure isotope components.

Numerous bands are observed in the 2300–2170 cm<sup>-1</sup> region because of the N–N stretching modes of Rh(NN)<sub>4</sub> and higher aggregates. These species have been characterized in the first rhodium–nitrogen matrix isolation study<sup>3</sup> and will not be discussed in detail here. The highest frequency product band below the dinitrogen stretching region is 1765.9 cm<sup>-1</sup>, with a site at 1771.5 cm<sup>-1</sup>. The <sup>15</sup>N counterparts for these bands are at 1729.5 cm<sup>-1</sup> and 1734.7 cm<sup>-1</sup>, respectively. No intermediate peaks are observed in the mixed or scrambled isotopic experiments. A broad, weak band grows in on annealing at 1707.1 cm<sup>-1</sup> in <sup>15</sup>N<sub>2</sub> experiments; the <sup>14</sup>N<sub>2</sub> counterpart for this band is believed to lie under the intense 1765.9 cm<sup>-1</sup> band at approximately 1765.1 cm<sup>-1</sup>. An intermediate band is observed in the scrambled isotopic experiment at 1735.9 cm<sup>-1</sup> with twice the intensity of the 1707.1 cm<sup>-1</sup> band, but no intermediate peak is found in the mixed isotopic experiment.

**Dinitrogen in Argon.** New absorptions from the co-deposition of rhodium with nitrogen in excess argon are summarized in Table 2. The region 1000–650 cm<sup>-1</sup> is shown in Figure 2

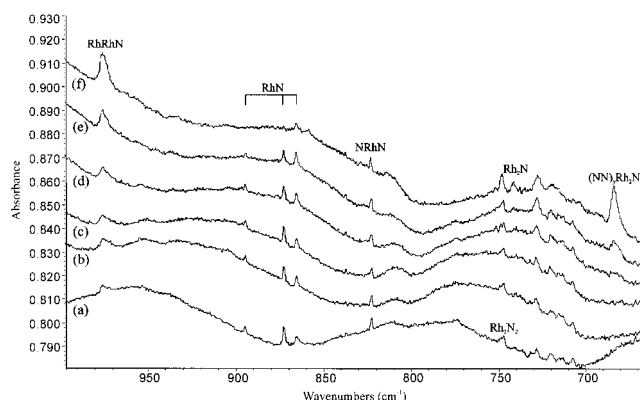


**Figure 2.** Infrared spectra in the 1000–650  $\text{cm}^{-1}$  region for laser ablated rhodium atoms co-deposited with nitrogen in argon (4%): (a) after 50 min deposition; (b) after annealing to 25 K; (c) after 25 min photolysis; (d) after annealing to 30 K; (e) after annealing to 35 K; (f) after annealing to 40 K.

for  $^{14}\text{N}_2$  in argon. Bands were observed in the nitride region at 975.6, 894.9, 872.9, 865.0, 822.8, 748.1, 741.5, 728.0, 720.3, 713.1, and 683.3  $\text{cm}^{-1}$  with  $^{15}\text{N}$  counterparts given in Table 2. The 975.6  $\text{cm}^{-1}$  band is very weak on deposition but grows throughout the annealing cycles. The 894.9, 872.9, and 865.0  $\text{cm}^{-1}$  bands are present on initial deposition and decrease steadily during annealing. The 822.8  $\text{cm}^{-1}$  absorption is unaffected by photolysis but decreases on annealing. Bands in the range 748.1–713.1  $\text{cm}^{-1}$  are weak, and the yields in the mixed and scrambled experiments are too low to identify intermediate components. Finally, the broad 683.4  $\text{cm}^{-1}$  band is not present initially but grows in throughout the annealing cycles. Only the 822.8  $\text{cm}^{-1}$  band shows an intermediate component in the scrambled isotopic experiment at 808.6  $\text{cm}^{-1}$ , which gives a 1:2:1 intensity pattern.

In the high-frequency region, bands due to the dinitrogen complexes  $\text{Rh}(\text{NN})_x$  ( $x = 1$  to 4) are included in Table 2. A much weaker, broad band is observed below the dinitrogen region at 1893.1  $\text{cm}^{-1}$  with an  $^{15}\text{N}$  counterpart at 1830.4  $\text{cm}^{-1}$ , which is not present initially but grows in during higher temperature annealings; a 1:2:1 intensity pattern is observed in the scrambled experiment with the intermediate peak at 1863.0  $\text{cm}^{-1}$ , and no intermediate band is observed in the mixed isotope experiment. A broad peak at 1775.1  $\text{cm}^{-1}$  grows throughout the annealing cycles but is unaffected by photolysis. No intermediate components are observed in either the mixed or scrambled isotopic experiments. A second broad band in the same region grows in at 1763.7  $\text{cm}^{-1}$ . The region is obscured in the scrambled isotopic experiment by the huge absorptions at 1775.1  $\text{cm}^{-1}$  and 1738.8  $\text{cm}^{-1}$  and so no intermediate bands can be observed, but an intermediate is observed in the mixed isotopic experiment with approximately half the intensity of the pure isotope bands at 1735.0  $\text{cm}^{-1}$ .

**Calculations.** Density functional theory calculations were performed on all of the proposed reaction products using the Gaussian 94 program.<sup>5</sup> The BPW91 functional<sup>6</sup> was employed in all calculations, and the D95\* and LanL2DZ effective core potential basis sets<sup>7</sup> were used for nitrogen and rhodium, respectively. Previous work has shown that pure density functionals and these basis sets are effective in calculating frequencies in good agreement with experiment for heavy transition metal atom reaction products.<sup>8</sup> The geometries and relative energies calculated for the rhodium nitride reaction products are listed in Table 3, and the calculated frequencies are listed in Table 4. The prominent species are shown schematically in Figure 3. These calculations are considered as

**TABLE 3: Relative Energies and Geometries Calculated for Rhodium Nitrides (BPW91/D95\*/LanL2DZ)**

molecule	state	relative energies (kJ/mol)	geometry ( $\text{\AA}$ , deg)
$\text{RhN}^a$	$1\Sigma^+$	0	RhN: 1.641
	$3\Sigma^-$	+182	RhN: 1.589
	$5\Sigma^-$	+208	RhN: 1.723
$\text{RhNN}$	$2\Sigma^+$	0	RhN: 1.882, NN: 1.146, $\angle\text{RhNN}$ : 180.0
$\text{RhNN}$	$2\Delta$	+2	RhN: 1.886, NN: 1.146, $\angle\text{RhNN}$ : 180.0
$\text{Rh}(\text{N}_2)$	$2A_1$	+45	RhN: 2.076, NN: 1.181, $\angle\text{NRhN}$ : 33.0
	$4B_1$	+136	RhN: 4.890, NN: 1.124, $\angle\text{NRhN}$ : 13.2
$\text{NRhN}$	$2B_1$	+397	RhN: 1.725, $\angle\text{NRhN}$ : 116.8
	$4A_2$	+437	RhN: 1.759, $\angle\text{NRhN}$ : 116.8
$\text{RhNN}^+$	$3\Delta$	+766	RhN: 2.003, NN: 1.129, $\angle\text{RhNN}$ : 180.0
$\text{Rh}_2\text{N}$	$2A_1$	0	RhRh: 2.764, RhN: 1.746, $\angle\text{RhNRh}$ : 104.7
	$4A_1$	+78	RhRh: 2.893, RhN: 1.772, $\angle\text{RhNRh}$ : 109.5
$\text{RhRhN}$	$2A'$	+162	RhRh: 2.362, RhN: 1.650, $\angle\text{RhRhN}$ : 134.5
	$4A'$	+187	RhRh: 2.474, RhN: 1.665, $\angle\text{RhRhN}$ : 113.9
$\text{Rh}_2(\text{N}_2)$	$3B_1$	0	RhRh: 2.445, RhN: 1.959, NN: 1.203
$\text{Rh}_2\text{NN}$	$3B_1$	+32	RhRh: 2.438, RhN: 1.995, NN: 1.169
	$1A_1$	+90	RhRh: 2.435, RhN: 1.988, NN: 1.170
$\text{RhRhNN}$	$3A''$	+45	RhRh: 2.428, RhN: 1.837, NN: 1.150 $\angle\text{RhRhN}$ : 96.7, $\angle\text{RhNN}$ : 180.0
	$1A_g$	+344	RhN: 1.665, RhRh: 2.452, $\angle\text{NRhRh}$ : 108.7
$\text{NRhRhN}$	$3B_g$	+330	RhN: 1.668, RhRh: 2.480, $\angle\text{NRhRh}$ : 110.6
	$5A_g$	+388	RhN: 1.686, RhRh: 2.574, $\angle\text{NRhRh}$ : 113.1
	$1A'$	0	RhN: 1.732, NO: 1.192, $\angle\text{RhNO}$ : 156.7
$\text{RhNO}$	$3A'$	+93	RhN: 1.859, NO: 1.202, $\angle\text{RhNO}$ : 128.1

<sup>a</sup> Calculated using MP2.

**TABLE 4: Frequencies and Intensities Calculated (BPW91/D95\*/LanL2DZ) for Selected Structures from Table 3**

molecule (state)	frequencies, $\text{cm}^{-1}$ (intensities, km/mol)
$\text{RhN}(1\Sigma^+)^a$	906.4 (1288)
$\text{RhNN}(2\Sigma^+)$	2100.8 (349), 440.6 (12), 217.8 (6)
$\text{RhNN}(2\Delta)$	2134.0 (277), 460.7 (6), 221.0 ( $2\times 6$ )
$\text{Rh}(\text{N}_2)(2A_1)$	1867.8 (138), 318.7 (6), 234.4 (6)
$\text{NRhN}(2B_1)$	940.0 (0), 824.6 (60), 317.5 (0)
$\text{NRhN}(4A_2)$	847.2 (19), 188.3 (11), 161.8 (30)
$\text{RhNN}^+(3\Delta)$	2243.0 (15), 335.4 (3), 230.7 ( $2\times 2$ )
$\text{RhRhN}(2A')$	1005.8 (82), 223.8 (0), 119.2 (1)
$\text{RhRhN}(4A')$	985.0 (52), 207.4 (1), 118.6 (3)
$\text{Rh}_2\text{N}(2A_1)$	861.2 (5), 748.4 (54), 151.2 (2)
$\text{NRhRhN}(1A_g)$	999.1 (0), 987.6 (169), 260.7 (0)
$\text{NRhRhN}(3B_g)$	974.3 (0), 935.0 (223), 220.1 (0)
$\text{Rh}_2(\text{N}_2)(3B_1)$	1708.5 (207), 521.8 (1), 512.9 (2)
$\text{Rh}_2\text{NN}(3B_1)$	1942.3 (286), 411.0 (3), 376.7 (0)
$\text{RhRhNN}(3A'')$	2092.1 (449), 502.9 (16), 301.0 (6)
$\text{RhNO}(1A')$	1787.5 (482), 624.2 (0), 141.5 (10)
$\text{RhNO}(3A')$	1662.2 (705), 576.2 (6), 255.6 (5)

<sup>a</sup> Calculated using MP2.

a first-order approximation to be used as a guide for vibrational assignments and provide starting points for subsequent ab initio calculations. SCF convergence was not possible for some molecules, and in these cases MP2 was used instead of DFT. These give results of similar quality, but direct comparison between calculated energies and frequencies are not meaningful.

## Discussion

Several new rhodium nitride species will be assigned based on isotopic shifts and DFT calculations.

**RhN.** The bands at 863.7  $\text{cm}^{-1}$  ( $^{14}\text{N}_2$ ) and 838.1  $\text{cm}^{-1}$  ( $^{15}\text{N}_2$ ) in a nitrogen matrix have an isotopic ratio of 1.03055, almost identical to the harmonic diatomic RhN ratio of 1.03060. This, and the fact that no intermediate peak is observed in the

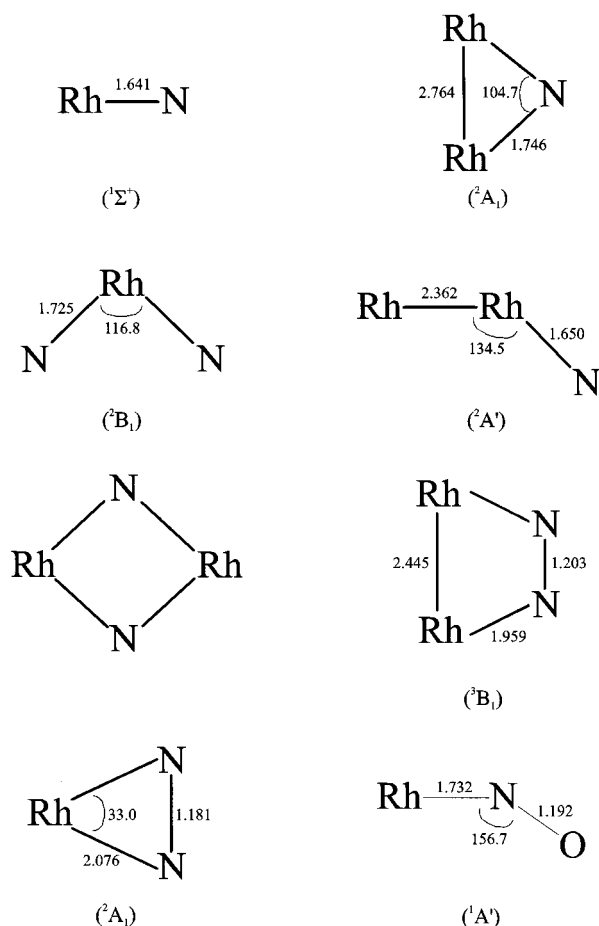


**Figure 3.** Optimized geometries for rhodium nitride products calculated using DFT (BPW91).

scrambled isotopic experiment, supports the assignment of these bands to the diatomic molecule RhN. The small discrepancy in the isotopic ratio is expected for normal cubic anharmonicity. This designation is incomplete as the molecule is embedded in solid nitrogen and most certainly has coordinated nitrogen molecules, i.e.,  $(\text{N}_2)_x\text{RhN}$  rather than RhN. Growth of the bands to 30 K in the nitrogen matrix must arise from the further association of Rh and N atoms. The characteristic absorption at  $1657.7\text{ cm}^{-1}$  due to an  $\text{N}_3$  radical confirms that N atoms are produced in these experiments.<sup>4,8,9</sup> However, in the argon matrix the uncomplexed molecule RhN should be observable. During the annealing cycles,  $\text{N}_2$  and perhaps even RhN can diffuse through the matrix and form the higher complexes, ultimately giving a band very close to that observed in the nitrogen matrix. Bands at  $894.9$ ,  $872.9$ , and  $865.2\text{ cm}^{-1}$  are observed on co-deposition of rhodium atoms with dinitrogen in argon. The  $^{15}\text{N}$  isotopic counterparts at  $868.4$ ,  $846.9$ , and  $839.8\text{ cm}^{-1}$  give ratios of 1.03052, 1.03070, and 1.03025, also close to the harmonic diatomic value. During annealing the two higher frequency bands decrease and are completely absent at 40 K where only the lowest frequency band, almost coincident with the value in the nitrogen matrix, remains at the final annealing cycle. Unfortunately, N–N stretching modes for the ligands could not be observed because of overlapping bands in this region. These bands show an overall decrease in intensity relative to the deposition spectrum, which is caused by consumption of RhN in reactions with other species in the matrix. The band at  $894.9\text{ cm}^{-1}$  is assigned to the uncomplexed RhN molecule. This is in agreement with the gas phase RhN fundamental at approximately  $896\text{ cm}^{-1}$ <sup>10</sup> and is somewhat higher than the  $826.5\text{ cm}^{-1}$  value for CoN in solid argon.<sup>2</sup>

DFT was used to calculate the singlet, triplet, and quintet states of RhN, but unfortunately SCF convergence could not be achieved for the singlet state. The calculations were repeated using MP2 instead, and the results are summarized in Tables 3 and 4. The singlet state is found to be of lowest energy, and the highest occupied orbitals are  $(\delta)^4(\sigma)^2$  to give a  $^1\Sigma^+$  ground state. This is in agreement with gas-phase studies of RhN, ab initio calculations, and photoelectron spectroscopy of  $\text{RhN}^-$ , which found  $^1\Sigma$  to be the lowest RhN state.<sup>10–12</sup> This result is different from CoN where  $^5\Delta$  was predicted to be the ground state.<sup>2</sup> The MP2 frequency,  $906.4\text{ cm}^{-1}$  is in very good agreement with the uncomplexed argon matrix frequency of  $894.9\text{ cm}^{-1}$ .

The MP2 results are also in good agreement with the bond length and frequency calculated recently,<sup>11</sup> within  $0.001\text{ \AA}$  and  $60\text{ cm}^{-1}$  of the ab initio values. The authors note the importance of relativistic corrections in obtaining the correct ordering of states, and this appears to be more important than the specific method used. It is also noted that the inclusion of an  $f$ -function on rhodium made no significant difference to the results, and so the absence of  $f$ -functions in the present study are not expected to detract from the quality or usefulness of the calculations.

**NRhN.** Evidence will be presented for rhodium dinitride. The 1:2:1 intensity pattern observed in the scrambled isotopic experiment at  $830.9$ ,  $816.2$ , and  $808.0\text{ cm}^{-1}$  (nitrogen matrix) and  $823.2$ ,  $808.6$ , and  $800.4\text{ cm}^{-1}$  (argon matrix) is indicative of a mode involving two equivalent nitrogen atoms. These observations support the assignment of these bands to the insertion product NRhN. The fact that the intermediate peak is observed in the mixed isotopic experiment but with only a ~1:1:1 ratio indicates that NRhN is formed by addition of a nitrogen atom to RhN as well as by the direct reaction between a rhodium atom and  $\text{N}_2$ . The 14/15 isotopic ratio of 1.02834 (nitrogen matrix) and 1.02813 (argon matrix) can be used to estimate the bond angle.<sup>13</sup> If the observed band corresponds to the  $\nu_1$  mode, then the bond angle is  $50^\circ$ , or  $130^\circ$  if the  $\nu_3$  mode is observed. The former angle would correspond to  $\text{Rh}(\text{N}_2)$ , a side-bound complex, and must be rejected as the Rh–N stretching modes would be of much lower frequency. The observed bands are therefore assigned to the  $\nu_3$  mode of NRhN, and the  $130^\circ$  estimated bond angle represents an upper limit on this quantity.<sup>13</sup> The triplet in the scrambled experiment is asymmetric; the central component is shifted down from the midpoint by  $3.3\text{ cm}^{-1}$ . This is due to coupling between the symmetric and antisymmetric motions in the  $^{14}\text{NRh}^{15}\text{N}$  molecule, which now have the same symmetry, and the downward shift indicates that the  $\nu_1$  mode is at higher frequency than the  $\nu_3$  mode. These results are different from the cobalt–nitrogen system where NCoN was not observed.

The DFT calculations for NRhN support assignment of the observed bands. The optimized doublet geometry has a bond angle of  $116.8^\circ$ . The calculated frequency for the  $\nu_3$  mode is within  $7\text{ cm}^{-1}$  of the argon matrix value, and the  $\nu_1$  mode is higher in frequency but is predicted to have negligible intensity, in excellent agreement with experiment. The quartet state is higher in energy than the doublet state, and the calculated frequencies are anomalous, and so  $^2\text{B}_1$  is identified as the ground state.

The dinitride NMN has been observed in matrix isolation experiments for other transition metals including niobium, chromium, manganese, and iron.<sup>8,14,15</sup> The bond angles and  $\nu_3$  frequencies for these molecules are  $102^\circ$ ,  $109^\circ$ ,  $127^\circ$ , and  $115^\circ$  and  $651.0$ ,  $883.3$ ,  $858.9$ , and  $934.8\text{ cm}^{-1}$ , respectively, and



clearly the 130° and 830.9 cm<sup>-1</sup> values observed for NRhN are in accord.

Finally, it is worth noting that NRhN does not conform to the qualitative geometry prediction based on Walsh-like rules for transition metal triatomics that anticipate a bent geometry for molecules with up to eighteen electrons but a linear geometry for nineteen or more electrons.<sup>16,17</sup> NRhN has nineteen valence electrons and so should be linear by this scheme, contrary to the experimental result. Deficiencies in this qualitative treatment have also been observed for the isoelectronic molecule OMnO and for OFeO, both of which adopt bent geometries.<sup>18,19</sup>

**RhRhN and Rh<sub>3</sub>N.** The molecule CoCoN was observed in the reaction between cobalt and nitrogen at 1016.6 cm<sup>-1</sup>.<sup>2</sup> It is reasonable to expect the Rh–N stretching mode of a rhodium analogue to be near 1000 cm<sup>-1</sup>. Bands at 1160.4 cm<sup>-1</sup> and 971.5 cm<sup>-1</sup> in the nitrogen matrix are candidates for this assignment because both exhibit doublets in the scrambled isotopic experiment, indicating the participation of only one nitrogen atom. The isotopic 14/15 ratios for these bands are 1.03303 and 1.03263, respectively, higher than the diatomic value of 1.03060, indicating a higher participation by nitrogen with respect to RhN. This is explained by assuming that the  $\nu(\text{Rh}-\text{Rh})$  and  $\nu(\text{Rh}-\text{N})$  stretching modes are essentially uncoupled, in which case the nitrogen atom can be treated as moving against a Rh<sub>2</sub> mass. Treating the molecule as pseudo diatomic and using the equation for a harmonic oscillator yields an isotopic ratio of 1.03265, in excellent agreement with the ratio for the 971.5 cm<sup>-1</sup> band, and in fair agreement for the ratio of the 1160.4 cm<sup>-1</sup> band.

DFT has been used to calculate the frequencies and optimum geometries for RhRhN in the doublet and quartet states, and the results are summarized in Tables 3 and 4. These calculations support assignment of the 971.5 cm<sup>-1</sup> band to the Rh<sub>2</sub>–N stretching mode of RhRhN. The energies of the optimized doublet and quartet states are within 25 kJ/mol of each other, which is within the margin of error for calculated energies, and so both must be considered. The calculated frequencies for both states are in very good agreement with experiment, the Rh<sub>2</sub>–N mode is calculated at 1005.8 cm<sup>-1</sup> and 955.6 cm<sup>-1</sup> for the doublet and quartet states, respectively. Both values are close to 971.5 cm<sup>-1</sup> and so the correct ground state cannot be determined with certainty, but the fit is slightly better for the doublet state, with respect to the energy and frequency. Both calculated values are much lower than the 1160.4 cm<sup>-1</sup> band and so its assignment to RhRhN must be rejected. Given the similar characteristics of its 1160.4 and 971.5 cm<sup>-1</sup> bands, it is likely that it is due to the larger cluster species Rh<sub>3</sub>N. The isotopic ratio for the 1160.4 cm<sup>-1</sup> band is marginally higher than for that assigned to RhRhN, indicating a greater participation by nitrogen in the mode, and this is consistent with the idea of a nitrogen atom moving against an even greater effective mass than Rh<sub>2</sub>.

It is interesting that these cluster species have higher frequencies than RhN despite their greater mass. The rhodium–nitrogen bond is evidently stronger than it is in the diatomic molecule, probably because antibonding electrons in RhN are incorporated into the rhodium–rhodium bond(s) to some extent. The reduced symmetry in the cluster species is another factor, i.e., the nonbonding  $\delta$  orbitals in the diatomic molecule, composed of the rhodium  $d_{x^2-y^2}$  and  $d_{xy}$  orbitals, acquire some bonding character in the cluster species.

RhRhN is also observed in the argon matrix at 975.6 cm<sup>-1</sup> (<sup>14</sup>N<sub>2</sub>) and 944.0 cm<sup>-1</sup> (<sup>15</sup>N<sub>2</sub>), but with only one-sixth of the intensity. In both matrixes, the bands grow on annealing but decrease on photolysis. The 1160.4 cm<sup>-1</sup> band is different: it

is destroyed during the first annealing cycle in a nitrogen matrix and is not observed at all in the argon matrix. The growth of RhRhN probably arises from addition of a rhodium atom to RhN, which is known to be present in high abundance, as the species diffuse through the softened matrix. The addition of nitrogen atoms to Rh<sub>2</sub> may also be involved, but the abundance of Rh<sub>2</sub> in these experiments is unknown and so the relative importance of this reaction cannot be determined. It is surprising for a higher cluster Rh<sub>3</sub>N to be depleted on annealing, as it should behave like RhRhN and increase as rhodium atoms diffuse through the matrix. It is likely that this species is consumed through reaction with the mobile nitrogen atoms.

The formation and characterization of rhodium dimers has been addressed in a previous matrix isolation study.<sup>20</sup> In that work the authors note the pronounced tendency of rhodium to dimerize to give binuclear complexes of N<sub>2</sub>, CO, and O<sub>2</sub>.<sup>3,21,22</sup> where the naked Rh<sub>2</sub> dimer was recognized from its UV/vis absorption spectrum. The trimer Rh<sub>3</sub> was also observed but only when considerably more metal was present in the matrix. Given that far less rhodium is produced by laser ablation compared to evaporation of a rhodium ribbon, it is likely that trinuclear species make only a minor contribution compared to dinuclear species in the present experiments. The relative intensities of the 1160.4 cm<sup>-1</sup> and 971.5 cm<sup>-1</sup> bands confirm this view, assuming the oscillator strengths of the two modes are of comparable magnitude.

**Rh<sub>2</sub>N.** The 738.9 and 732.5 cm<sup>-1</sup> bands in the nitrogen matrix have isotopic ratios of 1.03083 and 1.03154 for the two sites, respectively, close to but slightly higher than the diatomic harmonic value. The bands form doublets in the scrambled isotopic experiment, so a single nitrogen atom is involved. The diatomic molecule has already been assigned to the 863.5 cm<sup>-1</sup> band, and so an alternative explanation is required. The triatomic molecule RhNRh could give rise to an absorption with an isotopic ratio close to the diatomic ratio if the bond angle were close to 90°. This RhNRh molecule is a symmetrical isomer of Rh<sub>2</sub>N in addition to the asymmetric molecule RhRhN identified above. The 738.9 cm<sup>-1</sup> band is present initially but decreases rapidly on annealing, to be replaced by the lower frequency band. This behavior is attributed to increasing ligation of Rh<sub>2</sub>N during annealing, and the 732.5 cm<sup>-1</sup> band is due to the complexed form. This red shift on the more highly complexed molecule is analogous to that observed for RhN. In argon Rh<sub>2</sub>N absorbs at 741.5 cm<sup>-1</sup> with an isotopic ratio of 1.03086, though here it is much weaker and the effects of increasing complexation cannot be distinguished as they were for RhN. Increased complexation has another effect on the secondary site in addition to the frequency red shift, namely, a secondary isotope effect. In the mixed and scrambled isotopic experiments, the absorptions occur at 732.3 cm<sup>-1</sup> and 710.2 cm<sup>-1</sup>, shifted from the 732.5 and 710.1 cm<sup>-1</sup> values of the pure <sup>14</sup>N and <sup>15</sup>N bands. This is due to weak coupling between the motions of the molecule and those of the complexed dinitrogen giving rise to unresolved mixed isotopic multiplets that cause an apparent frequency shift. The Rh–N–Rh bond angle can be estimated from the isotopic ratio to be 84° for the  $\nu_1$  mode or 96° if it is the  $\nu_3$  mode that is observed.

The results of the DFT calculations for the doublet and quartet states of cyclic Rh<sub>2</sub>N are summarized in Tables 3 and 4. The <sup>2</sup>A<sub>1</sub> ground state has a calculated bond angle of 104.7°, which is near the experimental estimate for the  $\nu_1$  assignment. The calculated  $\nu_1$  frequency, 748.4 cm<sup>-1</sup>, is in good agreement with the observed band. The calculated rhodium–rhodium separation of 2.764 Å for the doublet state of Rh<sub>2</sub>N is considerably longer

than the value of 2.28 Å estimated for the Rh<sub>2</sub> dimer<sup>23</sup> but is comparable with bond lengths observed in numerous dirhodium complexes where values in the range 2.315–2.733 Å are known.<sup>24,25</sup> The calculated value lies just beyond this range, indicating that a relatively weak Rh–Rh bond is present in Rh<sub>2</sub>N. Also, the calculated  $\nu_2$  frequency of 151.2 cm<sup>-1</sup>, which is essentially the Rh–Rh stretching mode, is comparable with the values of 115–170 cm<sup>-1</sup> assigned to the Rh–Rh stretching mode in various dirhodium complexes.

It is interesting that two structural isomers of Rh<sub>2</sub>N are present in the matrix, cyclic Rh<sub>2</sub>N and the asymmetric species RhRhN. Our DFT calculations show the cycle to be considerably more stable. The presence of both species indicates that the reactions are under kinetic control rather than thermodynamic control, i.e., conversion between the two forms is not efficient. Clearly, asymmetric RhRhN molecules formed cannot overcome the energy barrier and rearrange to the more stable cyclic Rh<sub>2</sub>N isomer in the matrix at 8 K. The relative orientation of reactants may determine which product is formed, i.e., how a nitrogen atom approaches Rh<sub>2</sub> and how a rhodium atom approaches RhN.

The analogous molecule Co<sub>2</sub>N was observed in the cobalt system at 745.4 cm<sup>-1</sup> in a nitrogen matrix, very similar to the Rh<sub>2</sub>N band at 735.6 cm<sup>-1</sup>. DFT calculations predicted a doublet ground state,<sup>2</sup> also in line with the results for the rhodium analogue. It is interesting that these frequencies are so similar, considering the 68.4 cm<sup>-1</sup> difference between the diatomic frequencies. This can be explained by the force constants for these modes and the masses of the atoms involved. In the case of the diatomic molecules, the force constant for RhN is considerably higher than that for CoN, 582 Nm<sup>-1</sup> compared to 455 Nm<sup>-1</sup>. This more than compensates for the greater mass of rhodium, and RhN absorbs at a higher frequency than CoN. The force constant derived for the  $\nu_1$  mode of Rh<sub>2</sub>N is also greater than that of Co<sub>2</sub>N, 365 Nm<sup>-1</sup> compared to 308 Nm<sup>-1</sup>, but the difference is not as great as for the diatomic molecules and the greater mass of rhodium causes the  $\nu_1$  frequency of Rh<sub>2</sub>N to lie slightly lower than that of Co<sub>2</sub>N. In both cases the bonds are stronger for rhodium than for cobalt, consistent with the stronger  $\sigma$  bonding expected for the more expanded 4d orbitals compared with the compact 3d orbitals. Interaction between the  $\nu_1$  and  $\nu_2$  modes was ignored in these force constant calculations for Rh<sub>2</sub>N and Co<sub>2</sub>N, and the bond angles were taken to be 84° and 75° (the latter value was calculated using the isotopic data from ref 2). This trend does not hold for RhRhN and CoCoN however, as the force constants calculated treating the molecule as pseudo diatomic are 730 Nm<sup>-1</sup> and 762 Nm<sup>-1</sup>, respectively.

Another species related to Rh<sub>2</sub>N absorbs at 684.7 cm<sup>-1</sup> in a nitrogen matrix with a secondary site at 687.5 cm<sup>-1</sup>. This behaves like the dinitrogen complex of Rh<sub>2</sub>N at 732.5 cm<sup>-1</sup> in that it is very sharp, gives a doublet in mixed and scrambled isotopic experiments, has an almost identical isotopic ratio of 1.03149, and exhibits a secondary isotope effect with frequency shifts of -0.4 cm<sup>-1</sup> and +0.2 cm<sup>-1</sup> for the <sup>14</sup>N and <sup>15</sup>N peaks, respectively. However, unlike the 732.5 cm<sup>-1</sup> band it is present before annealing takes place, with approximately half the intensity of the 738.9 cm<sup>-1</sup> band, and continues to grow until the very last annealing cycle where the 732.5 cm<sup>-1</sup> band has already started to decrease in intensity. This band is attributed to the  $\nu_1$  mode of another dinitrogen complex of Rh<sub>2</sub>N which is more favorable than the complex that absorbs at 732.5 cm<sup>-1</sup>. The presence of two ligated forms of Rh<sub>2</sub>N showing red shifted frequencies is analogous to the behavior of RhN described above.

**Rh<sub>2</sub>N<sub>2</sub>.** The sharp band at 756.7 cm<sup>-1</sup> in a nitrogen film has an <sup>15</sup>N counterpart at 735.6 cm<sup>-1</sup> and an intermediate component at 745.0 cm<sup>-1</sup> in both the mixed and scrambled isotopic experiments. The overall intensity pattern is 1:2:1 in the latter case, indicating that two equivalent nitrogen atoms are involved. In the mixed isotopic experiment the central component has approximately the same intensity as either of the pure isotope bands. Because the 830.9 cm<sup>-1</sup> band has already been assigned to NRhN, and Rh(N<sub>2</sub>) is not a viable assignment, a dirhodium species is the most probable assignment for the 756.7 cm<sup>-1</sup> band. In the cobalt–nitrogen system a band was observed at 711.1 cm<sup>-1</sup>, which demonstrated a nearly diatomic shift and a 1:2:1 intensity triplet in both mixed and scrambled isotopic experiments.<sup>2</sup> This was assigned to the Co<sub>2</sub>N<sub>2</sub> rhombic ring, and given the similarities between cobalt– and rhodium–nitrogen systems, it is reasonable to expect that the analogous rhodium species will be present. Analogous bands are observed at 748.1 cm<sup>-1</sup> (<sup>14</sup>N) and 727.0 cm<sup>-1</sup> (<sup>15</sup>N) in an argon matrix, but this region in the scrambled isotopic experiment was too congested to be able to see an intermediate component.

DFT has been used to calculate the geometries and frequencies of three different geometrical isomers that are consistent with experimental observations; NRhRhN, Rh<sub>2</sub>N<sub>2</sub>, and RhN<sub>2</sub>NRh. The first of these has two terminal Rh–N bonds, and the calculated frequencies for the energetically competitive singlet and triplet states are over 950 cm<sup>-1</sup>, far too high to account for the observed bands. It proved impossible to calculate the latter two structures with DFT as SCF convergence could not be achieved; hence, Figure 3 does not show dimensions for Rh<sub>2</sub>N<sub>2</sub>. The calculations were repeated with MP2, but these also failed. In the absence of theoretical data there is no way to distinguish between Rh<sub>2</sub>N<sub>2</sub> and RhN<sub>2</sub>NRh, though comparison with the cobalt–nitrogen system suggests that the cyclic Rh<sub>2</sub>N<sub>2</sub> species is more likely. The isotopic ratio (1.02868) is less than the harmonic diatomic value (1.03060). This means that Rh<sub>2</sub>N<sub>2</sub> adopts a puckered ring because a planar ring is expected to give the diatomic ratio. The fact that the scrambled peak is observed in the mixed experiment indicates that one or more mechanisms involving nitrogen atoms from different dinitrogen molecules are involved in the formation of Rh<sub>2</sub>N<sub>2</sub>, namely the dimerization of RhN and/or the addition of a nitrogen atom to Rh<sub>2</sub>N. If these were the only reactions by which Rh<sub>2</sub>N<sub>2</sub> were formed, then the intensity pattern in the mixed isotope experiment would be 1:2:1. The observed pattern is closer to 1:1:1, so other routes involving a nitrogen molecule must also be important. These include the addition of a rhodium atom to Rh(N<sub>2</sub>), and/or the direct interaction of N<sub>2</sub> with Rh<sub>2</sub>. Rh(N<sub>2</sub>) was not observed in a nitrogen matrix and so the latter reaction is probably dominant. The observed annealing behavior is unusual, the bands are completely destroyed in the first annealing cycle. It is surprising that they do not grow, given the various ways in which the molecule can be made from precursors that are known to be present in the matrix.

**Rhodium Dinitrogen Complexes.** The dinitrogen complexes Rh(NN)<sub>x</sub> (x = 1 to 4) have been observed and characterized previously in both argon and nitrogen matrixes.<sup>3</sup> The dinitrogen groups were found to bind end-on to the metal atom in Rh(NN), Rh(NN)<sub>2</sub>, Rh(NN)<sub>3</sub>, and Rh(NN)<sub>4</sub> in linear, trigonal planar, and tetrahedral geometries, respectively. Only Rh(NN)<sub>4</sub> was observed in a nitrogen matrix, and isotopic substitution showed the complex to be reduced to D<sub>2d</sub> symmetry in this environment. The present BPW91 calculations predict a <sup>2</sup>Σ<sup>+</sup> ground state with a strong 2100.8 cm<sup>-1</sup> fundamental and a slightly higher <sup>2</sup>Δ state with a 2134.0 cm<sup>-1</sup> frequency. Previous B3LYP calculations<sup>26</sup>

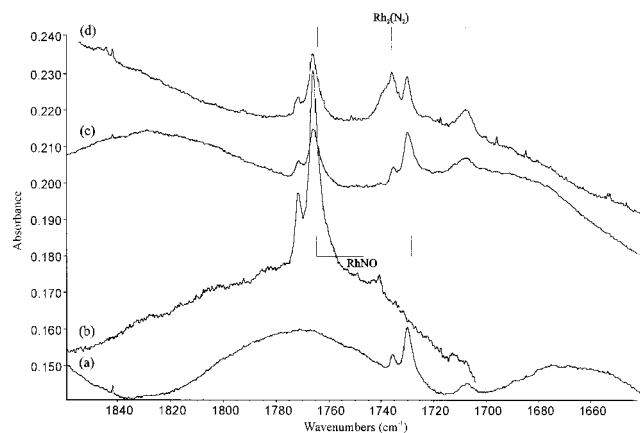


**Figure 4.** Infrared spectra in the 1860–1640  $\text{cm}^{-1}$  region for laser ablated rhodium atoms co-deposited with nitrogen after annealing to 34 K: (a)  $^{15}\text{N}_2$ ; (b)  $^{14}\text{N}_2$ ; (c)  $^{14}\text{N}_2 + ^{15}\text{N}_2$ ; (d)  $^{14}\text{N}_2 + ^{14}\text{N}^{15}\text{N} + ^{15}\text{N}_2$ .

probably correctly find the ground state as  $^2\Delta$  so the 2134.0  $\text{cm}^{-1}$  frequency will be used here. This calculated  $^2\Delta$  state frequency for RhNN is just below the previous<sup>3</sup> 2154  $\text{cm}^{-1}$  assignment and 2153.3  $\text{cm}^{-1}$  value observed here. The calculation requires a 1.009 scale factor to fit the observed frequency, which is in accord with scale factors for pure density functionals and transition metal compounds.<sup>27</sup>

The identification neutral RhNN is of interest for comparison to dinitrogen interacting with rhodium in  $\text{Al}_2\text{O}_3$  supported catalyst systems and on the metal surface.<sup>28–30</sup> A 2257  $\text{cm}^{-1}$  frequency is ascribed to the  $\text{N}_2/\text{Rh}/\text{Al}_2\text{O}_3$  surface species and a 2234  $\text{cm}^{-1}$  frequency to Rh(NN)(CO) on alumina.<sup>29,30</sup> If the 1.009 scale factor for our BPW91 calculation for RhNN applies to RhNN<sup>+</sup>, then a 2263  $\text{cm}^{-1}$  frequency is predicted for RhNN<sup>+</sup> in solid argon. Although this calibration is not exact, the 2257 and 2234  $\text{cm}^{-1}$  frequencies are clearly above neutral RhNN and near RhNN<sup>+</sup>, which suggests a partial positive charge on the Rh centers. A similar conclusion has been reached for the analogous carbonyl species.<sup>31</sup>

In the present study, no bands are observed in the low-frequency region in pure nitrogen but several are observed in argon. The 542.6  $\text{cm}^{-1}$  band is close to the 543  $\text{cm}^{-1}$  band observed in a nitrogen matrix in the original study, which was assigned to one of the deformation or skeletal stretching modes  $\text{Rh}(\text{N}_2)_4$  of  $T_2$  symmetry, but it cannot be due to  $\text{Rh}(\text{N}_2)_4$  because it decreases on annealing while the band assigned to the dinitrogen stretch for that species shows a marked growth on annealing. This and the other low-frequency bands are undoubtedly due to the various rhodium dinitrogen complexes, but making specific assignments to particular complexes would be futile in the absence of good isotopic data for these modes.

**Rh<sub>2</sub>(N<sub>2</sub>).** The region of the spectrum containing RhNO absorption (see below) is confused by the presence of another molecule at almost exactly the same frequency that is totally unrelated to the nitrosyl. Examination of Figure 4 shows a relatively weak, broad feature at 1707.1  $\text{cm}^{-1}$  in the  $^{15}\text{N}$  experiment, but no  $^{14}\text{N}$  counterpart is apparent. This band is also present in the scrambled isotope spectra, which also contains an intense broad band at 1735.9  $\text{cm}^{-1}$  that is twice as intense as the other band. These bands look like two components of a 1:2:1 triplet which could arise from an N–N stretching mode. In this case an isotopic shift of  $\sim 1.034$  is anticipated, and the  $^{14}\text{N}$  component would lie at  $\sim 1765$   $\text{cm}^{-1}$ , completely obscured by the broad nitrosyl band at 1765.9  $\text{cm}^{-1}$ . This interpretation is supported by the argon matrix spectra in Figure 5. Here, the mononitrosyl is present in very low yield in the

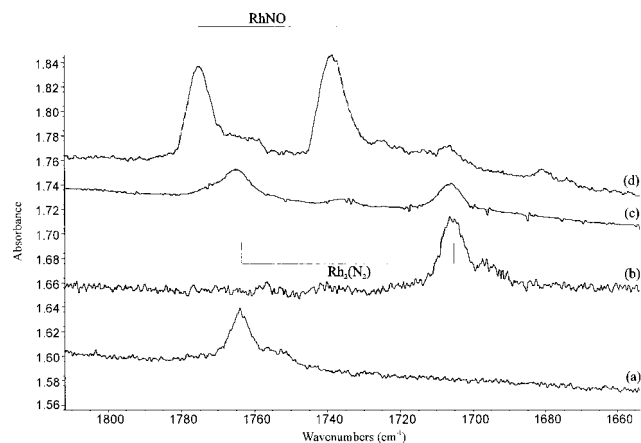


**Figure 5.** Infrared spectra in the 1820–1660  $\text{cm}^{-1}$  region for laser ablated rhodium atoms co-deposited with nitrogen in argon (4%) after annealing to 40 K. (a)  $^{14}\text{N}_2$ ; (b)  $^{15}\text{N}_2$ ; (c)  $^{14}\text{N}_2 + ^{15}\text{N}_2$ ; (d)  $^{14}\text{N}_2 + ^{14}\text{N}^{15}\text{N} + ^{15}\text{N}_2$ .

pure and mixed isotopic experiments and so the broad bands due to the N–N stretching mode at 1766.2  $\text{cm}^{-1}$  ( $^{14}\text{N}$ ) and 1705.9  $\text{cm}^{-1}$  ( $^{15}\text{N}$ ) are both observed. The mixed isotopic experiment shows these bands, as well as an intermediate component at 1734.1  $\text{cm}^{-1}$  that has grown in to a small extent during annealing. In the scrambled experiment, these peaks are overwhelmed by the strong nitrosyl absorptions and cannot be observed. This band does not track with any other bands in the spectrum. The most likely assignment for this band is to  $\text{Rh}(\text{N}_2)$ . Only one dinitrogen unit is involved, and RhNN has already been assigned at higher frequencies. Unfortunately, the frequency of 1867.8  $\text{cm}^{-1}$  calculated for  $\text{Rh}(\text{N}_2)$  is unacceptably high, and an alternative assignment must be considered. Given the abundance of dirhodium nitrides, a binuclear dinitrogen complex is suggested.

Several geometries with formula  $\text{Rh}_2\text{N}_2$  have been investigated using DFT, and the lowest energy structure is the  $\text{Rh}_2(\text{N}_2)$  parallelogram in a  $^3B_2$  state. The calculated frequency of 1708.5  $\text{cm}^{-1}$  is close enough to the experimental value of 1766.2  $\text{cm}^{-1}$  to support a tentative assignment.

**RhNO.** The broad intense band at 1765.9  $\text{cm}^{-1}$  in the nitrogen matrix has an  $^{15}\text{N}$  counterpart at 1729.5  $\text{cm}^{-1}$  to give a 14/15 isotopic ratio of 1.02105. This value is appropriate for the NO stretching vibration in a nitrosyl complex, i.e., the ratios for NiNO and CoNO are 1.0206 and 1.0218.<sup>2</sup> No intermediate components are observed in either the mixed or scrambled isotopic experiments, indicating that only one nitrosyl group is involved. The bands grow markedly on annealing as rhodium atoms and nitric oxide, present only as an impurity in these experiments, diffuse and react. The spectra for the pure, mixed, and scrambled isotopic experiments are shown in Figure 4. The mononitrosyl is also observed in the argon matrix at 1775.1  $\text{cm}^{-1}$  ( $^{14}\text{N}$ ) and 1738.8  $\text{cm}^{-1}$  ( $^{15}\text{N}$ ). These bands are very prominent in the scrambled isotopic experiment, as shown in Figure 4, but are barely detectable in the pure and mixed isotope experiments.

DFT has been used to calculate the geometry and frequencies for RhNO in both a singlet and triplet state, and the results are summarized in Tables 3 and 4. The singlet state is found to lie considerably lower in energy and to have a slightly bent geometry. The calculated NO stretching frequency of 1787.5  $\text{cm}^{-1}$  is in excellent agreement with the argon matrix value of 1775.1  $\text{cm}^{-1}$ .

**Reaction Mechanisms.** In the present and earlier laser ablation experiments with dinitrogen,<sup>2,4,14,15</sup> excess energy in



the laser ablated metal atoms dissociates enough dinitrogen to make free N atoms for the formation of metal nitrides and the  $N_3$  radical.<sup>9</sup> The sharp but weak  $N_3^-$  band<sup>9</sup> at  $2003.4\text{ cm}^{-1}$  was also observed in these experiments. At the laser power needed to ablate rhodium, there is sufficient laser plume intensity to photodetach most anions and neutralize cations that might be formed. Although we have observed charged species in dioxygen experiments,<sup>18,19</sup> the only charged species identified in the nitrogen work has been the azide anion.

## Conclusions

Laser ablated rhodium atoms co-deposited with pure nitrogen and nitrogen-doped argon at 10 K gave several new nitride species including RhN, NRhN,  $Rh_2N_2$ ,  $Rh_2N$ , and RhRhN. The rhodium system is found to be similar to the cobalt system<sup>2</sup> in several respects. The frequency shift for the diatomic molecule between the nitrogen and argon matrixes is the same for both metals, suggesting comparable effects of  $N_2$  complexation in pure dinitrogen, and the products MMN,  $M_2N$ , and  $M_2N_2$  are common to both systems with very similar frequencies. Force constant calculations for RhN and  $Rh_2N$  indicate that the bonds are stronger than for the cobalt analogues, but the opposite is true for the RhRhN molecule. Dirhodium species constitute a significant fraction of the reaction products. The low dinitrogen stretching frequency for  $Rh_2(N_2)$  and the long N–N bond calculated by DFT show that the interaction between the  $N_2$  unit and binuclear metal center is larger than in RhNN where  $N_2$  is bound to a single metal center. This suggests that a binuclear complex is better suited to weakening the strong N–N bond in a nitrogen fixation process.

DFT/BPW91(D95\* for nitrogen and LanL2DZ for rhodium) has been used to calculate the reaction products considered here, and in most cases it has proven to be very effective in reproducing experimental results; the calculated frequencies are consistently accurate to within a few tens of wavenumbers of the correct values. This level of accuracy makes it possible to choose between possible structures in making assignments with reasonable certainty. However, several of the DFT calculations failed, particularly those for singlet states of dirhodium species.

**Acknowledgment.** We appreciate financial support for this research from the University of Virginia and the National Science Foundation.

## References and Notes

(1) Bochmann, M. *Organometallics 1: Complexes with Transition Metal–Carbon  $\sigma$ -bonds*, Oxford Science Publications: Oxford, 1994.

- (2) Andrews, L.; Citra, A.; Chertihin, G. V.; Bare, W. D.; Neurock, M. *J. Phys. Chem. A* **1998**, *102*, 2561.
- (3) Ozin, G. A.; Vander Voet, A. *Can. J. Chem.* **1973**, *51*, 3332.
- (4) Hassanzadeh, P.; Andrews, L. *J. Phys. Chem.* **1992**, *96*, 9177.
- (5) *Gaussian 94, Revision B.1*. Frisch, M. J.; Trucks, G. W.; Schlegel, H. B.; Gill, P. M. W.; Johnson, B. G.; Robb, M. A.; Cheeseman, J. R.; Keith, T.; Petersson, G. A.; Montgomery, J. A.; Raghavachari, K.; Al-Laham, M. A.; Zakrzewski, V. G.; Ortiz, J. V.; Foresman, J. B.; Cioslowski, J.; Stefanov, B. B.; Nanayakkara, A.; Challacombe, M.; Peng, C. Y.; Ayala, P. Y.; Chen, W.; Wong, M. W.; Andres, J. L.; Replogle, E. S.; Gomperts, R.; Martin, R. L.; Fox, D. J.; Binkley, J. S.; Defrees, D. J.; Baker, J.; Stewart, J. P.; Head-Gordon, M.; Gonzalez, C.; Pople, J. A. (Gaussian, Inc., Pittsburgh, PA, 1995).
- (6) Becke, A. D. *Phys. Rev. A* **1988**, *38*, 3098. Perdew, P. J.; Wang, Y. *Phys. Rev. B* **1992**, *45*, 13244.
- (7) Dunning, T. H., Jr.; Hay, P. J. In *Modern Theoretical Chemistry*; Schaefer, H. F., III, Ed.; Plenum: New York, 1976. Hay, P. J.; Wadt, W. R. *J. Chem. Phys.* **1985**, *82*, 299.
- (8) Zhou, M. F.; Andrews, L. *J. Phys. Chem. A* **1998**, *102*, 9061.
- (9) Tain, R.; Facelli, J. C.; Michl, J. *J. Phys. Chem.* **1988**, *92*, 4073.
- (10) Fougere, S. G.; Balfour, W. J.; Qian, C. X. W., to be published.
- (11) Shim, I.; Mandix, K.; Gingerich, K. A. *J. Mol. Struct. Theochem.* **1997**, *393*, 127.
- (12) Li, X.; Wang, L.-S. *J. Chem. Phys.* **1998**, *109*, 5264.
- (13) Allavena, M.; Rysnik, R.; White, D.; Calder, V.; Mann, D. E. *J. Chem. Phys.* **1969**, *50*, 3399.
- (14) Andrews, L.; Bare, W. D.; Chertihin, G. V. *J. Phys. Chem. A* **1997**, *101*, 8417.
- (15) Chertihin, G. V.; Andrews, L.; Neurock, M. *J. Phys. Chem.* **1996**, *100*, 14609.
- (16) Weltner, W., Jr. *Ber. Bunsen-Ges. Phys. Chem.* **1978**, *82*, 80. Van Zee, R. J.; Brown, C. M.; Zeringue, K. J.; Weltner, W., Jr. *Acc. Chem. Res.* **1980**, *13*, 237.
- (17) Van Zee, R. J.; Hamrick, Y. M.; Li, S.; Weltner, W., Jr. *J. Phys. Chem.* **1992**, *96*, 7247.
- (18) Chertihin, G. V.; Andrews, L. *J. Phys. Chem. A* **1997**, *101*, 8547.
- (19) Chertihin, G. V.; Saffel, W.; Yustein, J. T.; Andrews, L.; Neurock, M.; Ricca, A.; Bauschlicher, C. W., Jr. *J. Phys. Chem.* **1996**, *100*, 5261.
- (20) Ozin, G. A.; Hanlan, A. J. L. *Inorg. Chem.* **1979**, *18*, 1781.
- (21) Hanlan, A. J. L.; Ozin, G. A. *J. Am. Chem. Soc.* **1974**, *96*, 6324.
- (22) Hanlan, A. J. L.; Ozin, G. A. *Inorg. Chem.* **1977**, *16*, 2858.
- (23) Cocke, D. L.; Gingerich, K. A. *J. Chem. Phys.* **1974**, *60*, 1958.
- (24) Boyar, E. B.; Robinson, S. D. *Coord. Chem. Rev.* **1983**, *50*, 109.
- (25) Bruno, G.; De Munno, G.; Tresoldi, G.; Lo Schiavo, S.; Piraino, P. *Inorg. Chem.* **1992**, *31*, 1538.
- (26) McKee, M. L.; Wooley, S. D. *J. Phys. Chem. A* **1997**, *101*, 5600.
- (27) Bytheway, I.; Wong, M. W. *Chem. Phys. Lett.* **1998**, *282*, 219.
- (28) Wang, H. P.; Yates, J. T., Jr. *J. Phys. Chem.* **1984**, *88*, 852.
- (29) Wey, J. P.; Neely, W. C.; Wooley, S. D. *J. Phys. Chem.* **1991**, *95*, 8879.
- (30) Wovchko, E. A.; Yates, J. T., Jr. *J. Am. Chem. Soc.* **1996**, *118*, 10250.
- (31) Zhou, M. F.; Andrews, L., to be published.